



CrossMark
 click for updates

Cite this: *RSC Adv.*, 2015, 5, 17049

Carbon nanotube cathodes covered on the cylindrical surface of a fiber

Xianqi Wei,^a Youzhang Zhu,^b Xianjun Xia,^a Xiaoli Wang,^{ab} Weihuan Liu^{*b} and Xin Li^b

Carbon nanotube (CNT) arrays were synthesized on the cylindrical waveguide surface of a quartz optical fiber by chemical vapor deposition (CVD) to serve as field emission cathodes. The roots of CNT arrays grew vertically on the fiber surface. Importantly, the change of fiber diameter affected the morphology of CNT tips. With the decrease in the fiber diameter, the gaps between CNT tips enlarged, which greatly improved the field emission properties of CNTs covered on cylindrical fiber surface. When the fiber diameter changed from 200 μm to 20 μm , the field enhancement factor (β) of CNT cathodes increased from 7823 to 11 631. Subsequently, the turn-on voltage (V_{to}) of CNTs cathodes decreased from 1290 V to 109 V, and the emission current density increased dramatically. In our work, the approach of synthesizing CNTs on optical fiber not only provides a route to improve β by simply changing fiber diameter, but also gives insight for a photo-assisted field emission nano cathode.

Received 20th November 2014
 Accepted 21st January 2015

DOI: 10.1039/c4ra14537b

www.rsc.org/advances

1. Introduction

Cold cathode materials of field emission serving as emitters, including diamonds,¹ micro-tip metals,² graphene film,³ and composite materials,⁴ have been developed efficiently in the past decades.⁵ As one of the most important cold cathode materials, carbon nanotubes (CNTs) have been widely studied as an ideal candidate for field emission emitters due to their high aspect ratio, high conductivity, good chemical stability and thermal stability. CNTs have been widely applied in field emission displays, electron beam lithography and travelling wave tubes.⁶ To improve the field emission properties of CNTs, the exploration of novel composites of CNT/graphene hybrids,⁷ three-dimensional CNTs⁸ and plasma treatment of CNTs⁹ have been reported for optimizing CNTs emitters. In the past few years, researchers have mainly focused on decreasing contact resistance or sharpening the tips of cathodes for enhancing field emission performance. Herein, we synthesized CNT arrays on the surface of naked optical fiber and improved the field emission properties of CNTs cathodes. In the previous research, CNTs were synthesized on various substrates, such as Si, Au and transparent substrates,⁶ and the majority of these substrates were flat substrates. Nevertheless, we present a method to synthesize CNTs on a cylindrical waveguide of optical fiber substrate. It is demonstrated that the morphology of CNTs can be changed by simply tuning the fiber diameter, resulting in the improvement of field emission properties.

Furthermore, well-aligned CNTs, which were synthesized on special substrates of functional materials, are a hot topic, in particular for photo-assisted field emission cathodes in which CNTs may have to be deposited on a waveguide. The fabrication of a cathode of CNTs covered on the fiber surface is a potential method for constructing a photo-assisted field-emission cathode.

2. Experiment

CNTs were synthesized on the fiber surface by chemical vapor deposition (CVD) using a carbon source of iron phthalocyanine. The substrate is a quartz optical fiber with a polymer coating layer and a cladding layer. To prepare the fiber substrate before CNTs growth, the polymer coating layer was removed with acetone, followed by ultrasonic treatment in ethanol and de-ionized water (DI water). Then, the quartz optical fiber was corroded in dilute hydrofluoric acid (~ 13 wt% HF). The corrosion rate was approximately 20 μm to 25 μm per hour. The fiber diameter was reduced from 220 μm cladding diameter to the desired size by controlling the corrosion time. After ultrasonic treatment, the prepared fiber was used as substrate for the growth of CNT arrays. Our synthesis apparatus is a variable-temperature horizontal furnace (Thermcraft). The growth of CNT arrays followed a typical chemical vapor deposition (CVD) process with the pyrolysis of iron phthalocyanine. The metal phthalocyanines in this method of growth process acted not only as a carbon source but also as a metallic catalyst,¹⁰ which has been reported in a previous work.^{11–13} The growth temperature range was from 800 $^{\circ}\text{C}$ to 900 $^{\circ}\text{C}$ for 15 min. The flow rates of hydrogen and argon were 25 sccm and 60 sccm, respectively. The morphological and microstructure

^aSchool of Science, Xi'an Jiaotong University, Xi'an, Shaanxi, China, 710049

^bDepartment of Microelectronics, School of Electronics and Information Engineering, Xi'an Jiaotong University, Xi'an, Shaanxi, China, 710049. E-mail: wei.wxq@163.com; Fax: +86 29 82663343; Tel: +86 29 82663343

characterization of synthesized CNTs were investigated using a JSM-7000F scanning electron microscope (SEM), a Tecnai F30 G² field-emission transmission electron microscope (TEM), a D8 ADVANCE X-ray diffractometer with Cu K α radiation source ($\lambda = 1.5406 \text{ \AA}$) at a scanning rate of 0.5 deg s^{-1} and a HORIBA JOBIN YVON Raman Spectroscopy with an excitation wavelength of 514 nm.

3. Results and discussion

Fig. 1 shows the schematic illustration of carbon nanotube arrays covered on a fiber surface, and Fig. 2(a) is a scanning electron micrograph (SEM) image showing the densely packed CNTs that grew on the surface of the fiber with a length of 6–8 μm . Detailed structures of CNTs were characterized by TEM. The synthesized CNTs were multi-walled nanotubes. Fig. 2(b) and (c) are a low-magnification TEM image and a high-resolution TEM image, respectively, showing that the diameters of CNTs were 20–100 nm. As shown in Fig. 2(c), the distance between two lattice fringes is measured to be 0.34 nm, which is close to the spacing of a (002) crystal plane of graphite ($d_{(002)} = 0.34 \text{ nm}$), and no structure defects are observed. Besides, the Raman pattern of CNTs was obtained by Raman spectroscopy with an excitation of 514 nm, as shown in Fig. 2(d). The disorder-induced D band appears at 1352 cm^{-1} , and the tangential mode G appears at 1585 cm^{-1} . The D and G bands corresponded to the main Raman feature of multi-walled CNTs. The ratio of intensities of D and G bands was less than 1 indicating a high quantity of structure defects,¹⁴ which corresponded to the TEM images. The second-order peak of the 2D band, which is caused by the double resonant Raman scattering with two-phonon emissions, approximates at 2700 cm^{-1} . As shown in Fig. 3, the XRD pattern of CNT arrays on the fiber surface exhibited a sharp (002) Bragg reflection at about $2\theta = 26.2^\circ$, which was derived from the ordered arrangement of the concentric cylinders of graphitic carbon. Moreover, the peak centered at 2θ of about 21.9° indicates the SiO₂ content corresponding to the quartz fiber substrate.

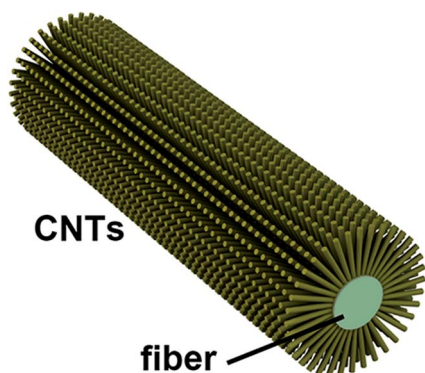


Fig. 1 Schematic illustration of carbon nanotube (CNT) cathodes covered on a fiber surface.

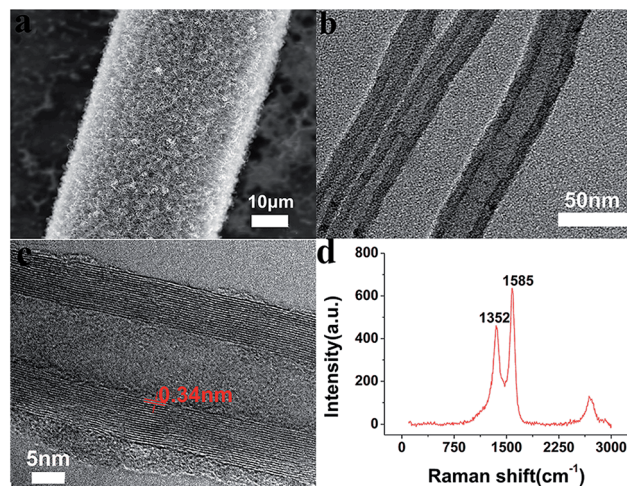


Fig. 2 (a) The scanning electron micrograph (SEM) image of carbon nanotube (CNT) cathodes covered on the surface of a fiber substrate. (b) A low-magnification TEM image of carbon nanotubes (CNTs) and (c) a high-resolution TEM image of a carbon nanotube (CNT). (d) The Raman spectrum of synthesized carbon nanotubes (CNTs), with the disorder-induced D band at 1352 cm^{-1} , the tangential mode G at 1585 cm^{-1} , and the second-order peak of the 2D band, which is caused by the double resonant Raman scattering with two-phonon emissions at approximately 2700 cm^{-1} .

Fig. 4(a) is a cross-section SEM image, which presents that CNTs on the fiber surface have uniform length and roots density. Fig. 4(c) is a high-magnification SEM image of the CNT roots obtained from the circled area in Fig. 4a. The roots vertically aligned and got tightly packed on the fiber surface. Fig. 4(b) shows the surface morphology of the CNT tips, and Fig. 4(d) shows the magnified top view SEM image. Though the dense roots of CNTs arrays vertically attached on the fiber surface, the tips radiated outward along the radial direction of fiber substrate. The gaps between the CNT tips were clear, in contrast to the morphology of the roots. Therefore, the change of fiber diameter affected the morphology of the tips of CNTs, which covered the cylindrical surface of the optical fiber substrate showing uniform lengths and root density. With the decrease in the fiber diameter, the gaps between tips enlarged, which resulted in the decrease of density of the tips. Thus, the distance between the neighbouring CNT tips was greatly

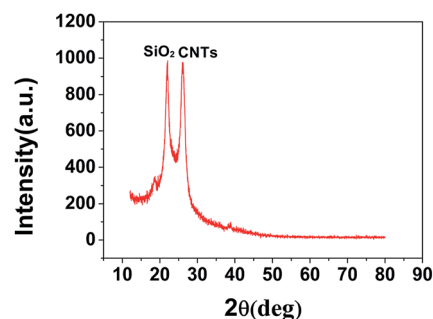


Fig. 3 The X-ray diffraction pattern of carbon nanotube (CNT) cathodes covered on a fiber surface.

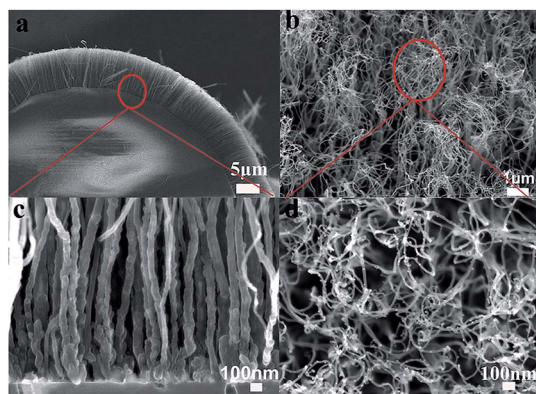


Fig. 4 (a) The cross-section SEM image of CNTs covered on fiber surface, (b) SEM top view image of the surface morphology of the CNTs tips, (c) a magnified view of the roots, and (d) a magnified top view of the tips.

dependent on the fiber substrate. The distance of the tips of CNTs could be changed by simply tuning the fiber diameter, as shown in Fig. 5. Fig. 5(a) and (b) show the low-magnification SEM images of CNTs covered on the surface of fibers with diameters of 200 μm and 20 μm . The surface of CNTs had several remarkable cracks on the fiber substrate with diameter of 20 μm because the gap between tips of nanotubes enlarged on a smaller diameter curve surface. Fig. 5(c) and (d) present the magnified top view SEM images of the surface morphology of the CNTs recorded from the marked area in Fig. 5a and b. Fig. 5(e) is a cross-section image of CNTs covered on the cylindrical surface of a 200 μm diameter fiber, and Fig. 5(f) shows

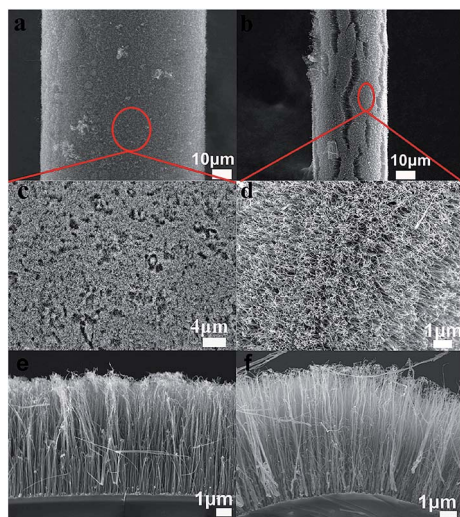


Fig. 5 (a) and (b) show the low-magnification SEM images of CNTs covering the fiber surfaces with diameters of 200 μm and 20 μm , respectively. (c) A top view SEM image showing the surface morphology of CNTs covering the 200 μm diameter fiber surface. (d) A top view SEM image showing the surface morphology of CNTs covering the 20 μm diameter fiber surface; (e) and (f) are the cross-section images of CNTs covering the surface of fiber substrate with the diameter of 200 μm and 20 μm , respectively.

CNTs on the surface of the fiber with a smaller diameter of 20 μm . Compared to the several voids of CNT tips on the 200 μm diameter fiber surface, separated CNT tips distinctly covered on the curve surface of the 20 μm diameter fiber substrate.

Fig. 6 shows the field emission measurement results of CNTs covering the fiber substrates with diameters of 200 μm , 100 μm , 40 μm , 30 μm and 20 μm . Field emission measurements were performed in a vacuum chamber with pressure less than 5×10^{-5} Pa. The anode-to-cathode spacing was 400 μm . A DC bias voltage with an increasing step of 50 V was applied between the anode and the cathode to establish an electrostatic field. Fig. 6(a) is the current density *versus* voltage (J - V) curves. For the fiber substrate with the diameter of 20 μm , the CNT cathode performed the minimum turn-on voltage V_{to} (defined as the applied voltage required to generate an emission current density of 1 mA cm^{-2}), yielding the maximum emission current at a lower applied voltage compared to the others. When the diameter of fiber substrate decreased from 200 μm to 20 μm , the turn-on voltage V_{to} was decreased and the emission current density increased at the same applied voltage with the decrease in fiber diameter; the field enhancement factor β of CNTs increased from 7823 to 11 631, and the turn-on voltage V_{to} decreased from 1290 V to 109 V; corresponding data is shown in Table 1.

It is a well-known fact that the field enhancement factor (β) of nano cathodes has a significant effect on field emission properties. Actually, if the cathode surface has a high point or a protrusion, electrons may be extracted at a considerably lower applied field. This is because the electric lines of force converge

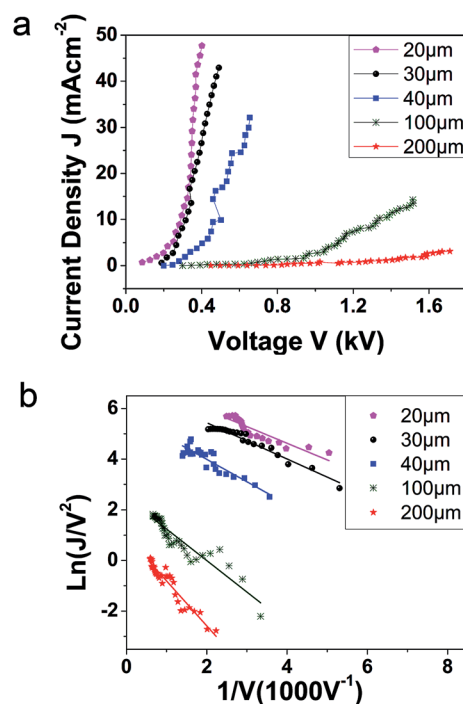


Fig. 6 The field emission properties of CNTs covered on the surfaces of the fibers with diameters of 20 μm , 30 μm , 40 μm , 100 μm and 200 μm . (a) Plots of emission current density (J) vs. applied voltage (V), and (b) is the corresponding Fowler-Nordheim (F-N) plots.

Table 1 The turn-on voltage (V_{to}) and the field enhancement factor (β) of CNTs cathodes covered on the surfaces of the fibers with diameters of 20 μm , 30 μm , 40 μm , 100 μm and 200 μm

Diameter (μm)	20	30	40	100	200
V_{to}	109	190	270	730	1290
β	11 631	11 338	10 562	9247	7823

at a sharp point and the physical geometry of the tip provides a field enhancement, which is expressed as a field enhancement factor (β).⁵ However, the dense individual tips are very close to each other, and there will be a screening effect on the top of the tips. The screening effect can weaken the field enhancement factor β resulting in a high applied field to extract electrons into vacuum, which is a drawback for the field emission properties of cathodes. Thus, the field enhancement factor β is greatly dependent on the surface morphology of the cathodes. Our approach for fabricating a cylindrical structure of CNT cathode can change field emission properties by simply tuning fiber diameter. Vertically aligned CNTs, which covered the cylindrical surface, radiated outward along the radial direction of the fiber. When the fiber diameter changed, the morphology of the CNTs tips would be changed. The gaps between tips enlarged while the fiber diameter decreased. The field enhancement factor β increased subsequently. It is beneficial for improving the field emission properties resulting from a decreased screening effect, as shown in Fig. 6 and Table 1. The field enhancement factor β was calculated from the slope and intercept of the Fowler–Nordheim (F–N) plots in Fig. 6(b). The turn-on voltage V_{to} and the field enhancement factor β of CNTs covered on different diameter fiber surfaces are listed in Table 1. The field enhancement factor β of CNTs increased from 7823 to 11 631 and the turn-on voltage V_{to} decreased from 1290 V to 109 V when the diameter of fiber substrate decreased from 200 μm to 20 μm .

4. Conclusion

Cylindrical cathodes of carbon nanotubes (CNTs) were successfully synthesized on a quartz fiber surface by a chemical vapor deposition (CVD) method. The vertically aligned CNTs on the fiber surface were multi-walled nanotubes, with the length of 6–8 μm and the diameter of 20–100 nm. The morphology of CNT cathodes on the fiber surface can be controlled by tuning the size of the diameter of the quartz fiber. With the fiber diameter decreased, the gaps between CNT tips enlarged, resulting in the change of the surface morphology of CNTs on fiber surface. Field emission investigation revealed that the field enhancement factor (β) greatly depended on the diameter of fiber substrate. When the fiber diameter decreased from 200 μm to 20 μm , the field enhancement factor of the CNT cathodes increased from 7823 to 11 631, and the turn-on voltage V_{to} decreased from 1290 V to 109 V subsequently. The novel high-performance cylindrical CNT cathode on the waveguide

surface could simply improve field emission properties by tuning fiber diameter.

Acknowledgements

This work was financially supported by the National Natural Science Foundation of China (grant nos 91123018, 61172041, 61172040, 50975226, and 60801022), the National 863 Key Project of Panel Displays (grant no. 2008AA03A314), and the Fundamental Research Funds for the Central Universities.

References

- W. P. Kang, J. L. Davidson, Y. M. Wong and K. Holmes, Diamond vacuum field emission devices, *Diamond Relat. Mater.*, 2004, **13**(4), 975–981.
- P. Hommelhoff, Y. Sortais, A. Aghajani-Talesh and M. A. Kasevich, Field emission tip as a nanometer source of free electron femtosecond pulses, *Phys. Rev. Lett.*, 2006, **96**(7), 077401.
- J. L. Qi, X. Wang, W. T. Zheng, H. W. Tian, C. Q. Hu and Y. S. Peng, Arplasma treatment on few layer graphene sheets for enhancing their field emission properties, *J. Phys. D: Appl. Phys.*, 2010, **43**(5), 055302.
- J. H. Deng, R. T. Zheng, Y. M. Yang, Y. Zhao and G. A. Cheng, Excellent field emission characteristics from few-layer graphene–carbon nanotube hybrids synthesized using radio frequency hydrogen plasma sputtering deposition, *Carbon*, 2012, **50**(12), 4732–4737.
- N. S. Xu and S. E. Huq, Novel cold cathode materials and applications, *Mater. Sci. Eng.*, 2005, **48**(2), 47–189.
- W. I. Milne and M. T. Cole, *25th IVNC*, Jeju, Korea, IP3, 2012, pp. 8–11.
- J. H. Deng, R. T. Zheng, Y. M. Yang, Y. Zhao and G. A. Cheng, Excellent field emission characteristics from few-layer graphene–carbon nanotube hybrids synthesized using radio frequency hydrogen plasma sputtering deposition, *Carbon*, 2012, **50**(12), 4732–4737.
- W. Choi and I. Lahiri, Novel design considerations for high efficiency carbon nanotube field emitters, *25th IVNC*, Jeju, Korea, 2012, p. 30.
- S. G. Yu and J. Y. Kim, Structure change and field emission of carbon nanotubes treated by plasma, *25th IVNC*, Jeju, Korea, 2012, p. 190.
- J. Song, M. Sun, Q. Chen, J. Wang, G. Zhang and Z. Xue, Field emission from carbon nanotube arrays fabricated by pyrolysis of iron phthalocyanine, *J. Phys. D: Appl. Phys.*, 2004, **37**(1), 5.
- X. Li, F. Ding, W. Liu, Y. He and C. Zhu, Luminescence uniformity studies on dendrite bamboo carbon submicron-tube field-emitter arrays, *J. Vac. Sci. Technol., B*, 2008, **26**(1), 171–174.
- S. Zuo, X. Li, W. Liu, Y. He, Z. Xiao and C. Zhu, Field emission properties of the dendritic carbon nanotubes film embedded with ZnO quantum dots, *J. Nanomater.*, 2010, **2011**(2011), 382068.

- 13 H. Liu, H. Ma, W. Zhou, W. Liu, Z. Jie and X. Li, Synthesis and gas sensing characteristic based on metal oxide modification multi wall carbon nanotube composites, *Appl. Surf. Sci.*, 2012, **258**(6), 1991–1994.
- 14 E. F. Antunes, A. O. Lobo, E. J. Corat, V. J. Trava-Airoldi, A. A. Martin and C. Veríssimo, Comparative study of first- and second-order Raman spectra of MWCNT at visible and infrared laser excitation, *Carbon*, 2006, **44**(11), 2202–2211.